Natural Resources Canada / Ressources naturelles Canada

GEOLOGICAL SURVEY OF CANADA
OPEN FILE 7841

Geological setting and geochemistry of the ca. 2.6 Ga Snow Island Suite in the central Rae Domain of the Western Churchill Province, Nunavut

T.D. Peterson, C.W. Jefferson, and A. Anand

2015

Canada

GEOLOGICAL SURVEY OF CANADA
OPEN FILE 7841

Geological setting and geochemistry of the ca. 2.6 Ga Snow Island Suite in the central Rae Domain of the Western Churchill Province, Nunavut

T.D. Peterson, C.W. Jefferson, and A. Anand

2015

doi:10.4095/296599

This publication is available for free download through GEOSCAN (http://geoscan.nrcan.gc.ca/).

Recommended citation
Peterson, T.D., Jefferson, C.W., and Anand, A., 2015. Geological setting and geochemistry of the ca. 2.6 Ga Snow Island Suite in the central Rae Domain of the Western Churchill Province, Nunavut; Geological Survey of Canada, Open File 7841, 1 .zip file. doi:10.4095/296599

Table of Contents

Introduction

The contents of this open file are geochemical data on *ca*. 2.6 Ga intrusive (Snow Island Suite) and extrusive (Pukiq Lake Formation) rocks collected during the GEM1-Uranium project (Jefferson et al., 2011a,b). Detailed interpretations of igneous processes and structural/stratigraphic ramifications, will be presented in future publications. Geochronological results are listed in Jefferson et al. (2015a,b).

The term Snow Island Suite (SIS) was first employed by Peterson and Lee (1995), for the type plutonic area around Snow Island, western Dubawnt Lake (NTS65N, 100 km south of the west edge of Fig. 1a). The SIS records voluminous, widespread magmatism throughout the Rae Province (Fig. 1a inset), primarily from ca 2.61 to 2.59 Ga. The extent of the SIS was first noted within the central Rae by LeCheminant and Roddick (1991) who documented felsic intrusive and volcanic rocks near 2.6 Ga. Subsequent geochronological studies have confirmed that the intrusive suite extends throughout the entire length of the Rae Province, from the southern Rae (Davis et al., 2015) through Dubawnt Lake (Peterson, 2006) and the central Rae (Kjarsgaard et al., 1997; Pehrsson et al., 2013; N. Wodicka, pers. comm. 2015; this study), westward across the Chantrey Mylonite Zone to the Thelon Front (Davis et al., 2014), and to the far northeast Rae at Melville and Boothia peninsulas (Hinchey et al., 2011; Corrigan et al., 2013).

The SIS has mafic and felsic components ranging from olivine websterite to diorite, and quartz diorite to granite respectively. The mafic component of the suite has not been recognized in most other studies but is prominent in the current study area, and at Dubawnt Lake (Peterson, 2006). The dominant member of the felsic component in all areas of the Rae Province where the suite is recognized is a coarse, potassium feldspar porphyritic monzonite to monzogranite with kspar “megacrysts” to 5 cm. Tonalite, grey-brown weathering equigranular granodiorite, and red to orange-pink weathering leucogranite with minor pegmatite also occur in large (10+ km) exposures.

The Pukiq Lake Formation name was proposed by Peterson et al. (2014) for a fine grained quartz-feldspar porphyry exposed in a 10 km wide oval area of outcrop on the west side of NTS 65O (LeCheminant et al., 1981) dated at 2610 +11/-13 Ma by LeCheminant and Roddick (1991). The reference areas for the mafic component of the Pukiq Lake Formation (PL) are located on the south side of the Amer Belt. Sample 11JP271A is located 5 km south of Amer Lake and is intercalated with dacite; sample 11JP524A is 30 km south-southeast of Umiujalik Lake.

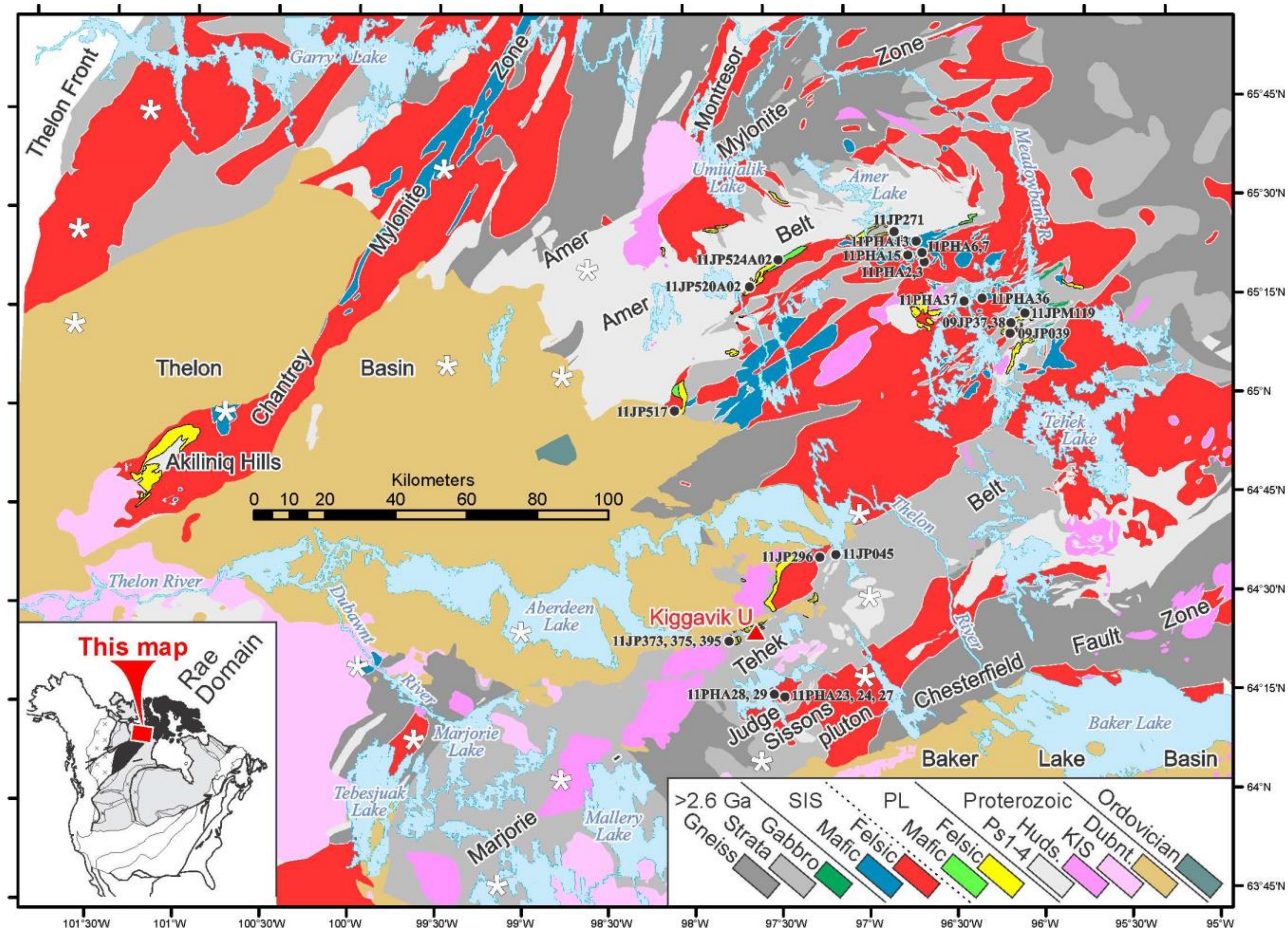

Figure 1a. Sample locations (black dots) in basement around the northeast Thelon Basin are shown with respect to simplified map units extracted from the database of Jefferson et al. (2015a, b). Snowflakes show locations of strong aeromagnetic highs (Fig. 1b) inferred to be deep plutons of the Snow Island Suite (SIS). Some of these are not exposed, especially those beneath the Thelon Basin. The balance of the SIS shown in red is interpreted as thin sheets (see text). Legend abbreviations: >2.6 Ga: gneiss = banded gneiss and highly foliated granitoid rocks; strata = volcano-sedimentary belts; gabbro = synvolcanic intrusions; SIS = Snow Island Suite intrusive rocks; mafic = ultramafic to dioritic phases; felsic = granodioritic to granitic phases; PL = Pukiq Lake Formation volcanic rocks (PL in text); mafic = basalt; felsic = dacite to rhyolite; Proterozoic Ps1-4 = regional Paleoproterozoic sequences described by Rainbird et al. (2010). Huds. = Hudson Suite granodiorite to granite and Martell Syenite; KIS = Kivalliq Igneous Suite undifferentiated mafic to felsic intrusive and extrusive rocks; Dubnt. = Dubawnt Supergroup comprising alluvial sedimentary rocks and ultrapotassic volcanic and hypabyssal intrusive rocks; Ordovician = fossiliferous limestone.

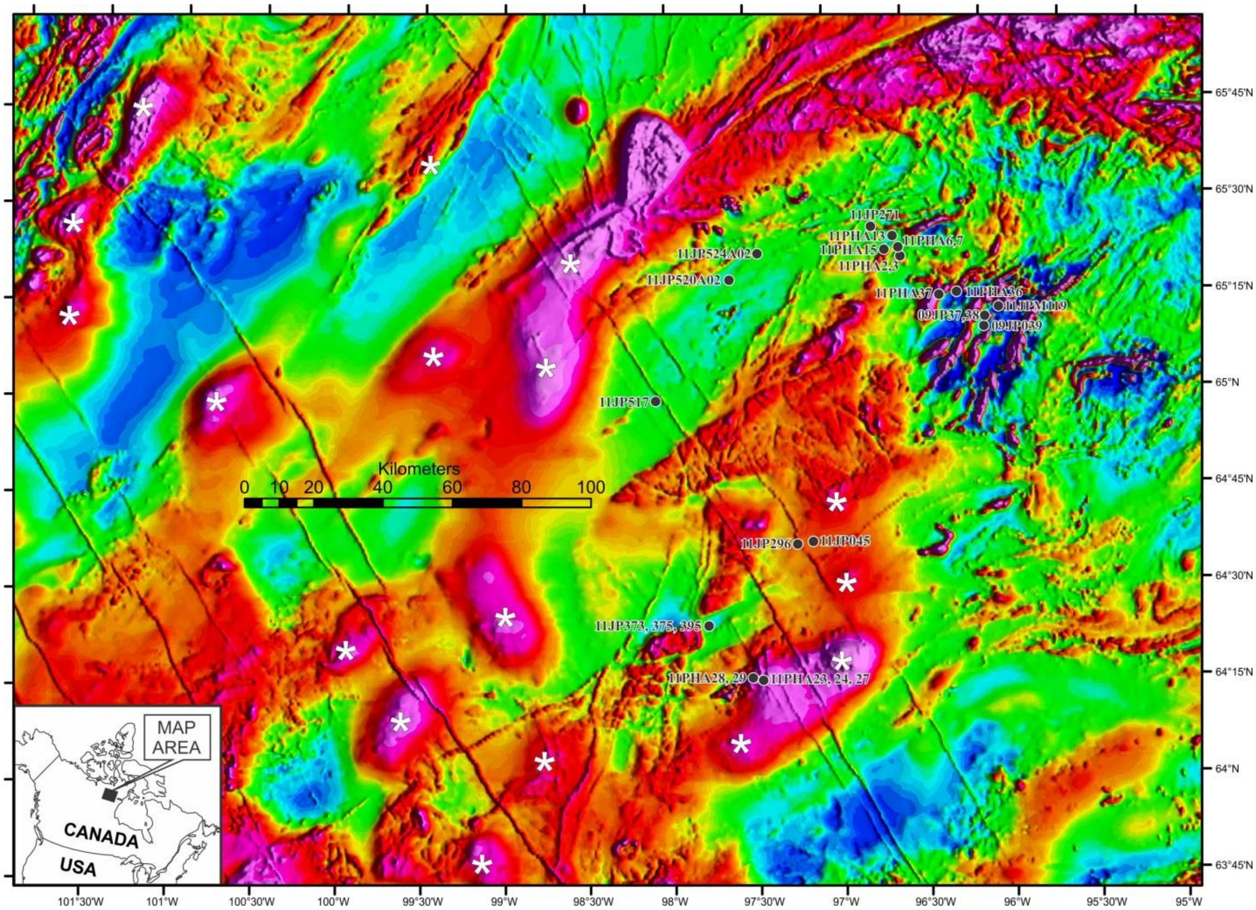

Figure 1b. Sample locations in basement around the northeast Thelon Basin, shown with respect to total magnetic field in the same area as Fig. 1a. Snowflakes located on peak aeromagnetic anomalies are in the same places as and explained in Fig. 1a for comparison with surface geology (see text).

Geological and geophysical context

In the GEM1-U area, the Judge Sissons Pluton (located in Fig. 1a) (2606 +4/-3 Ma, unpublished data of C. Roddick in Hadlari et al., 2004) is our type example of a felsic intrusion. It consists of an agmatitic border phase (Fig. 2) surrounding a pluton core that consists of potassium feldspar porphyritic monzonite, with amphibole and biotite defining a weak to moderate foliation. A subset of the felsic intrusions are geophysically manifested as domal aeromagnetic anomalies, but the majority are magnetically transparent. The domal anomalies have been interpreted in 3D as a product of deeply rooted, steep-sided bodies (Tschirhart et al., 2013a, 2013b), with disseminated magnetite and mafic enclaves being responsible for the magnetic susceptibility. The magnetically transparent granite bodies are now recognized as tectonic sheets transported over both Neoarchean and Paleoproterozoic supracrustal assemblages (Kjarsgaard et al., 1997). They were partly eroded to form windows exposing the underlying strata (Thomas, 2012; Pehrsson et al., 2013; Jefferson et al., 2015a, b). Examples include the informally named Tehek Lake plutonic complex (Schau et al., 1982) and large exposures of foliated granite along the Meadowbank River, both previously interpreted as deep plutons of Archean and/or Proterozoic age with inclusions of both Archean and Proterozoic supracrustal rocks (Tella, 1994; Zaleski, 2005). One reason why previous mappers thought the SIS is Proterozoic is the common lack of deformation fabrics. Ashton (1988) explained the lack of fabric in SIS intrusions by strain partitioning. Intense deformation in the SIS is restricted to basal shear planes of klippe (Pehrsson et al., 2013) and along major strike-slip shear zones like the Amer and Slave-Chantrey (LeCheminant et al., 1984; Tella, 1994).

The sampled mafic intrusive bodies are consistently associated with intense aeromagnetic anomalies, but these are smaller (only 1 to 10 km in diameter) than the felsic bodies, which can be over 100 km in length. It is uncertain if these small plutons are part of the system of tectonically emplaced felsic sheets or are *in situ* intrusions. In some cases they appear to be mingled with and/or form the cores of the large felsic complexes. Mafic rocks also form inclusions in agmatite at the contact zones of large plutons (Fig. 2). SIS mafic intrusions are distinguished from synvolcanic Archean diorite and gabbro by their circular magnetic signatures, in contrast to the elongate to linear signatures of the older rocks, and in general are only weakly deformed (see sample descriptions). All of the mafic bodies contain

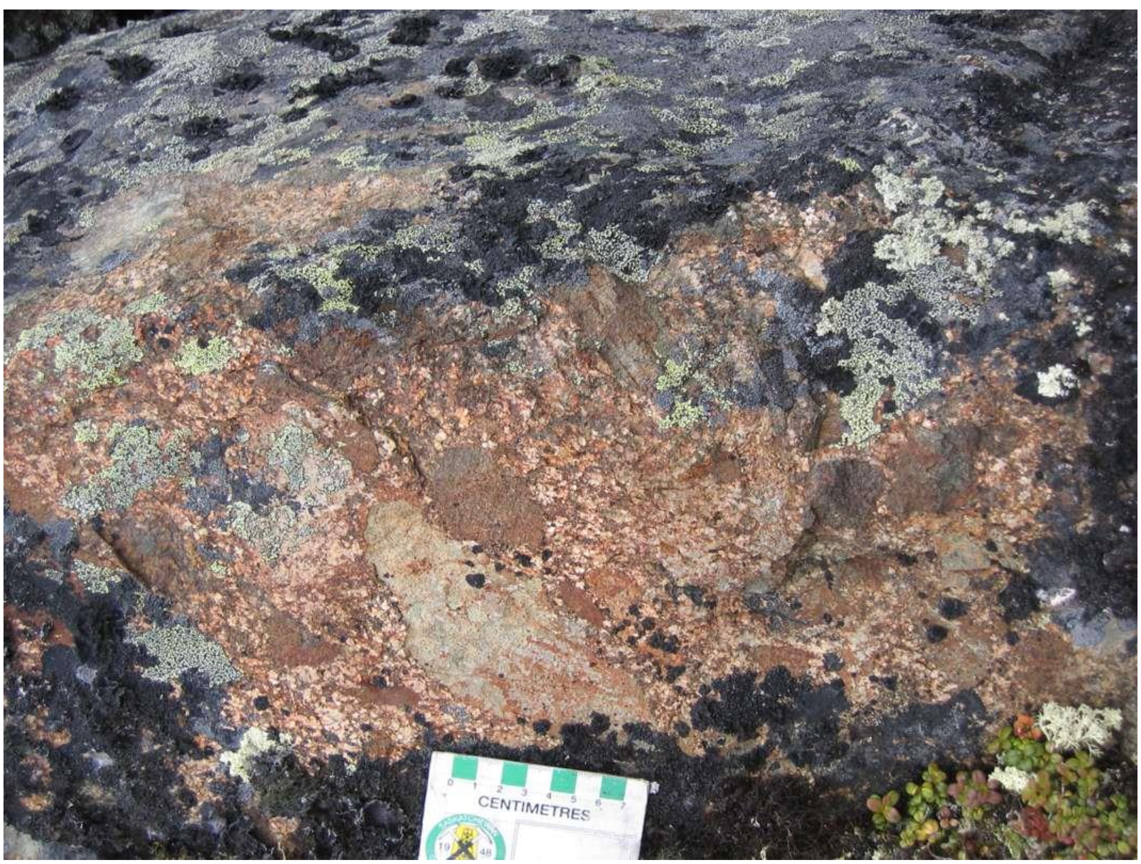

Figure 2. Metasedimentary, basaltic, and gabbroic to dioritic inclusions in contact agmatite of monzogranite (Judge Sissons pluton). Note the dark matrix of the youngest intrusive phase, which may have resulted from mafic-felsic mingling.

primary hornblende phenocrysts, which are the dominant carriers of magnetite in the rocks. Examples include an orbicular gabbro southeast of north Meadowbank River (11PHA-36, below) and numerous gabbroic intrusions immediately south of the Amer belt, where Zaleski (2005) also mapped a massive to weakly foliated, hornblende-bearing olivine websterite.

Felsic volcanic equivalents of the SIS (Pukiq Lake Formation, PL) are challenging to map because they are mostly aphanitic dacite to rhyolite that is tectonically interleaved with Paleoproterozoic Amer and Ketyet River groups, which contain foliated sericitic quartzite members that can resemble silicic volcanic rocks (McEwan, 2013; Jefferson et al., 2015a, b). Epiclastic rocks have been identified only in the Bong prospect area (west of the Kiggavik uranium prospect) where they are intercalated with PL rhyolite. The thinly bedded character of the epiclastic rocks is very similar in appearance to some distal metagreywacke units of the Woodburn Lake group, and may have been overlooked elsewhere.

SIS mafic volcanic rocks have only been found in three or four localities (along the southeast flank of Amer Belt), two of which were analyzed in this study (localities 11JP271 and 11JP524). At 11JP271 a rhyolite is structurally intercalated with the mafic volcanics, and these rocks appear to grade compositionally from one to the other. The mafic volcanic rocks are not porphyritic, may locally exhibit flow-top breccias, and can also be silicified. The SIS mafic rocks are distinguished from the younger tholeiitic basalt of the Amer and Ketyet groups by the lack of carbonate alteration and by intercalation with felsic volcanic rocks, which are lacking from the Amer and Ketyet groups.

The PL is preserved discontinuously, typically only along the edge of Paleoproterozoic belts where it forms the underlying basement. It is also locally incorporated as clasts in conglomerate at the base and top (McEwan, 2013; Jefferson et al., 2015a,b) of the Paleoproterozoic quartzite unit (Ps1 of Rainbird et al., 2010). In some places the rhyolite intervenes between SIS diorite to granite and the overlying quartzite; in others it is sandwiched between metagreywacke of the Woodburn Lake group and the quartzite. The Paleoproterozoic strata are also structurally interleaved with the underlying Neoarchean rocks, including both the Woodburn Lake group and the PL volcanics (McEwan, 2013). The rhyolite and rare basalt commonly forms a key marker unit between the older Archean Woodburn Lake group and the Paleoproterozoic quartzite, which is particularly useful for determining facing directions to help unravel the complex deformation. The multiple folds and shearing have locally imparted a very strong L-S fabric to the rhyolite, including comminution of both feldspar and quartz phenocrysts as part of local mylonitization processes. Detailed studies have confirmed that this is indeed both a rhyolite and locally a mylonite, especially because the mylonitized units can be traced to less deformed places which preserve lapilli tuff textures (e.g. sample 11JPM119) as well as round quartz eyes and equant feldspar phenocrysts.

Selected Sample Descriptions

Sample locations are included in the elemental data spreadsheet, and identified in figures 1a and 1b. Digital scans and descriptions of selected sawn hand samples, and some outcrop photographs, appear in the following section. Samples in the data spreadsheet were classified and color-coded based on geochemical groupings as described below.

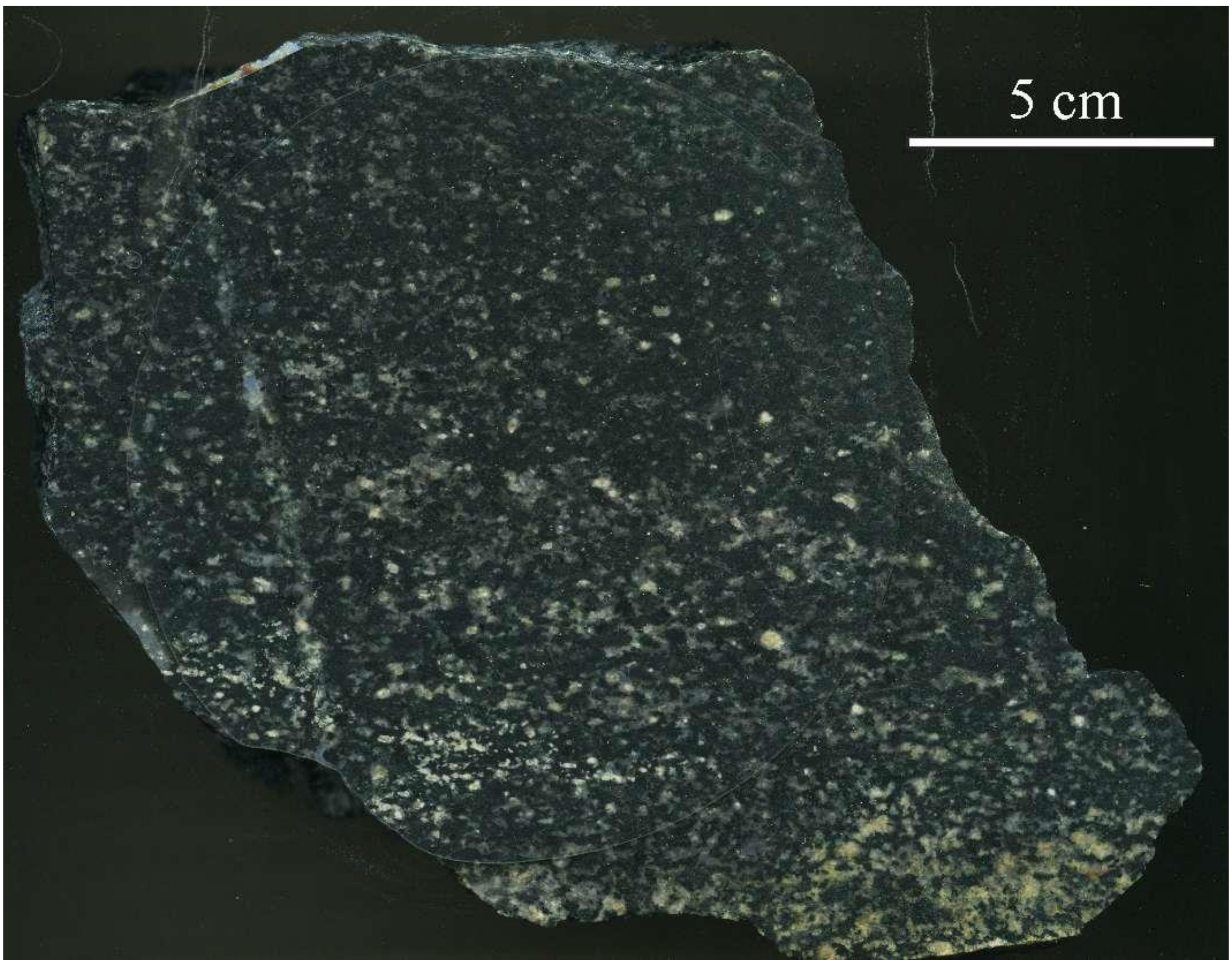

Figure 3. Sawn hand sample 11PHA-02.

<u>11PHA-02 (gabbro)</u> The specimen is a weakly foliated, mesocratic hornblende-plagioclase rock with no relic pyroxenes and irregular opaques included in amphibole. Euhedral apatite to 0.5 mm is abundant and is always included in, or in contact with amphibole. Minor chloritization of amphibole, and alteration of plagioclase cores, is present.

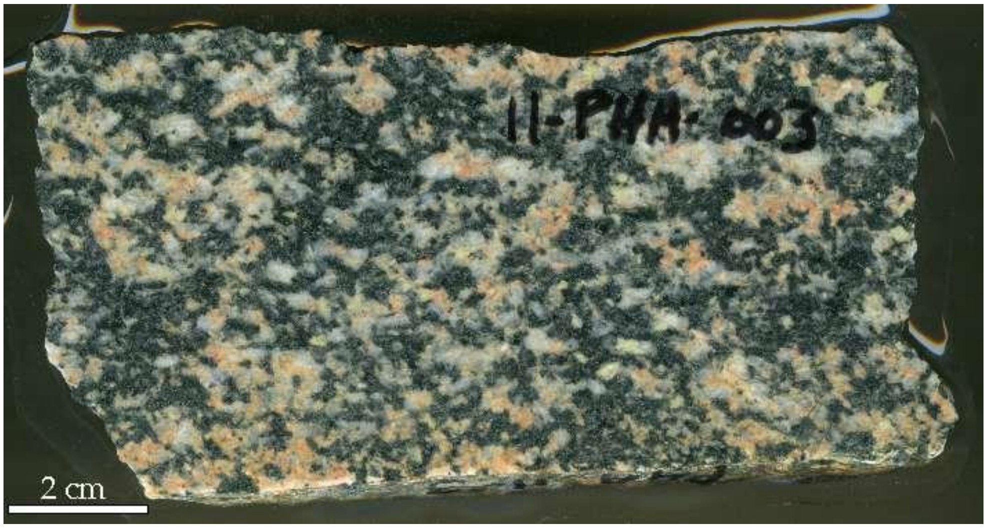

Figure 4. Sawn hand sample 11PHA-03.

11PHA-03 (diorite) The specimen (nondeformed) has cumulate plagioclase texture with intercumulate quartz + hornblende + apatite + opaques.

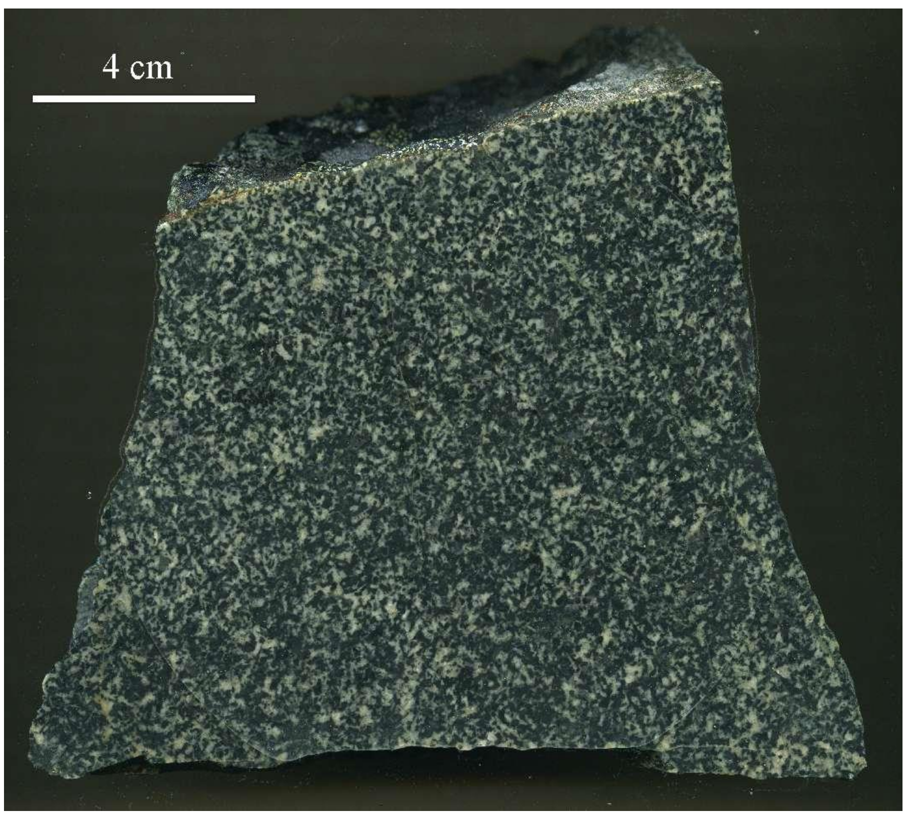

Figure 5. Sawn hand sample 11PHA-06.

11PHA-06 (gabbro) The specimen is a nondeformed hornblende and plagioclase cumulate with some hornblende occurring as cm-scale oikocrysts with inclusions of euhedral plagioclase and apatite, and of chlorite/amphibole that are probably altered pyroxene. Euhedral magnetite to 0.3 mm occurs outside the hornblende.

Figure 6. Outcrop area of 11PHA-07, showing massive, nonfoliated, dark-weathering gabbro.

<u>11PHA-07 (gabbro)</u> The specimen is nondeformed, and is a weakly plagioclase cumulate rock with irregular hornblende containing irregular apatite to 1 mm. Sparse opaques are associated with amphibole. The plagioclase is nearly all altered. The irregular nature of the apatite and amphibole give an impression of recycled, partially resorbed crystals.

Figure 7. Mesocratic intrusive sample (diorite) 11PHA-13.

11PHA-13 (diorite) The specimen is a nondeformed, plagioclase + hornblende + phlogopite cumulate (phlogopite<<amphibole) with interstitial plagioclase and quartz; opaque minerals are absent except for secondary blebs in phlogopite. The phlogopite and cumulate plagioclase are strongly altered but intercumulate plagioclase is mostly unaltered.

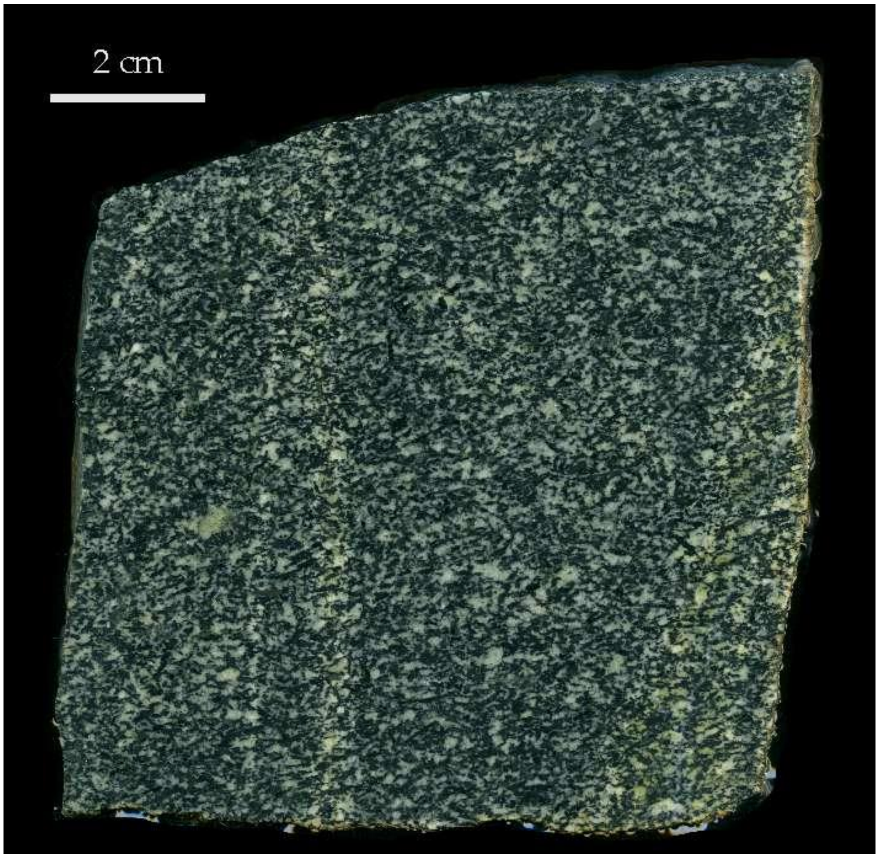

Figure 8. Intrusive gabbro (amphibole cumulate) sample 11PHA-15.

Figure 9. Quartz tonalite segregations in gabbro, site of sample 11PHA-15.

<u>11PHA-15 (gabbro)</u> The outcrop is dominated by a melanocratic, coarse grained hornblende cumulate locally with prominent, reflective, oikocrystic amphibole. Decimeter-scale segregations and veins of quartz tonalite with amphibole and biotite are common throughout the outcrop. Magnetite is included in the amphibole. The intercumulate matrix is dominated by plagioclase, with secondary epidote, and minor biotite. Quartz and alkali feldspar, if present, are in trace quantities.

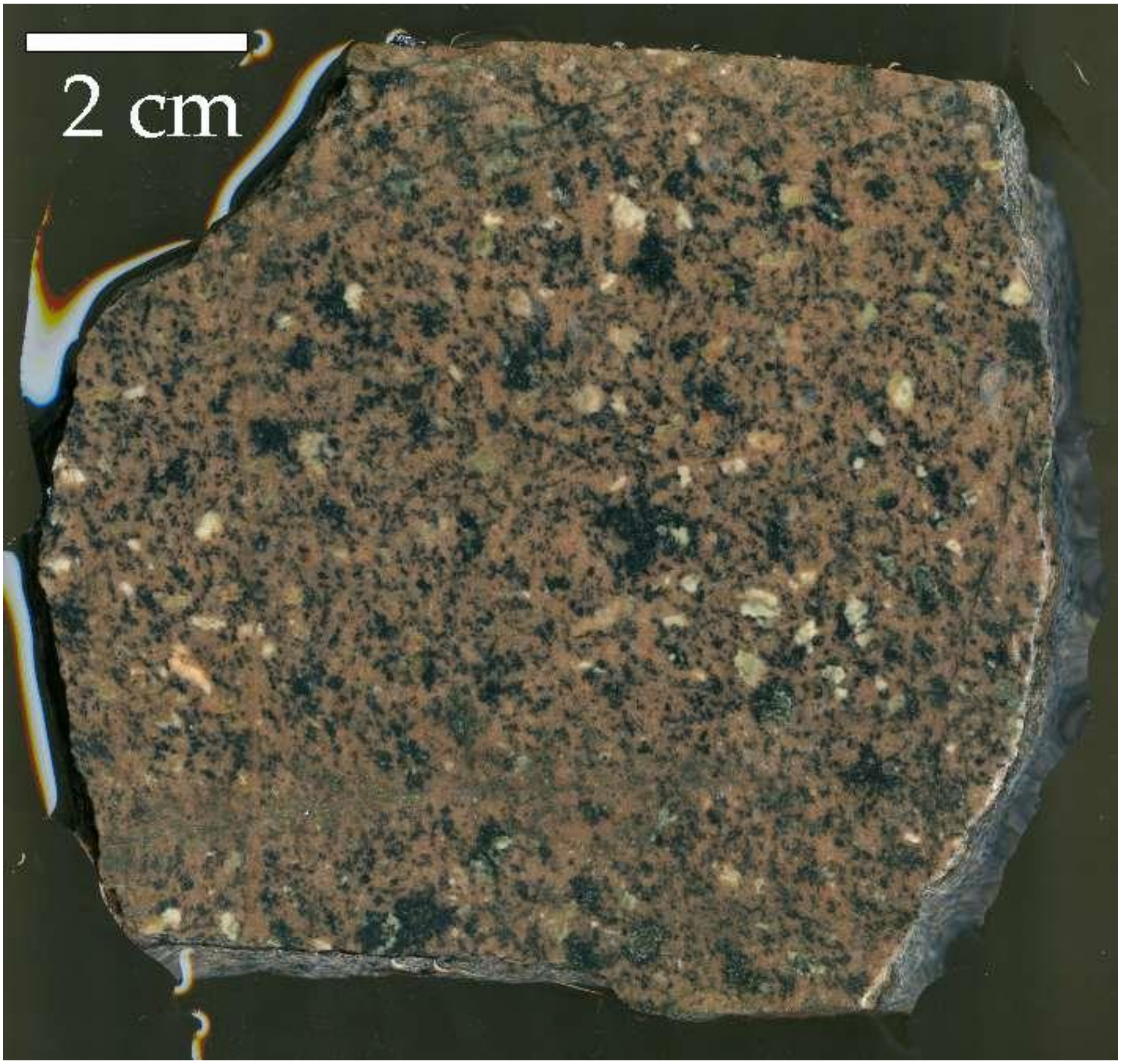

Figure 10. Sawn hand sample 11PHA-23.

11PHA-23 (granodiorite) (thin section unavailable; see -24). The hand specimen is nonfoliated with a weak extension lineation (at a high angle to the depicted surface above) which consists of sparse, irregular, altered plagioclase crystals to 5 mm and irregular green-black amphibole to 1 cm in a brown-pink weathering matrix consisting of subequal amounts of plagioclase, alkali feldspar, and quartz.

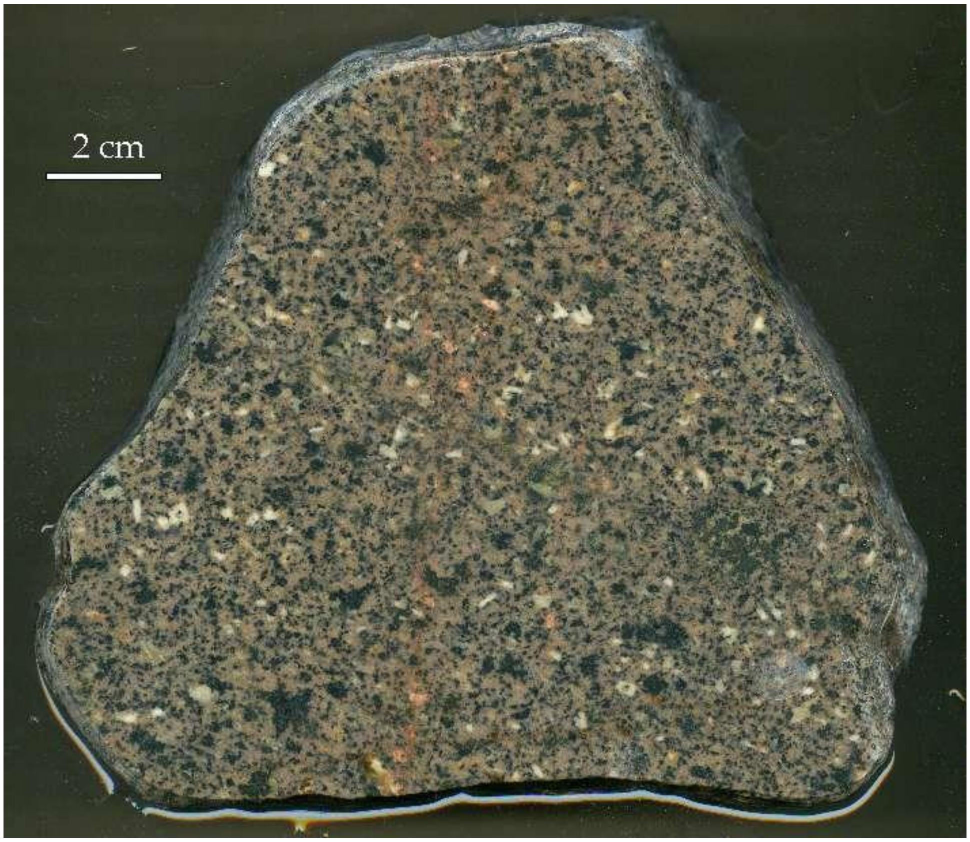

Figure 11. Sawn hand sample 11PHA-24.

11PHA-24 (granodiorite) The specimen, nondeformed, consists of highly altered plagioclase crystals to 8 mm in a matrix of unaltered quartz + plagioclase + untwinned alkali feldspar with interstitial apatite + dark brown-green-blue pleochroic amphibole and dark brown biotite.

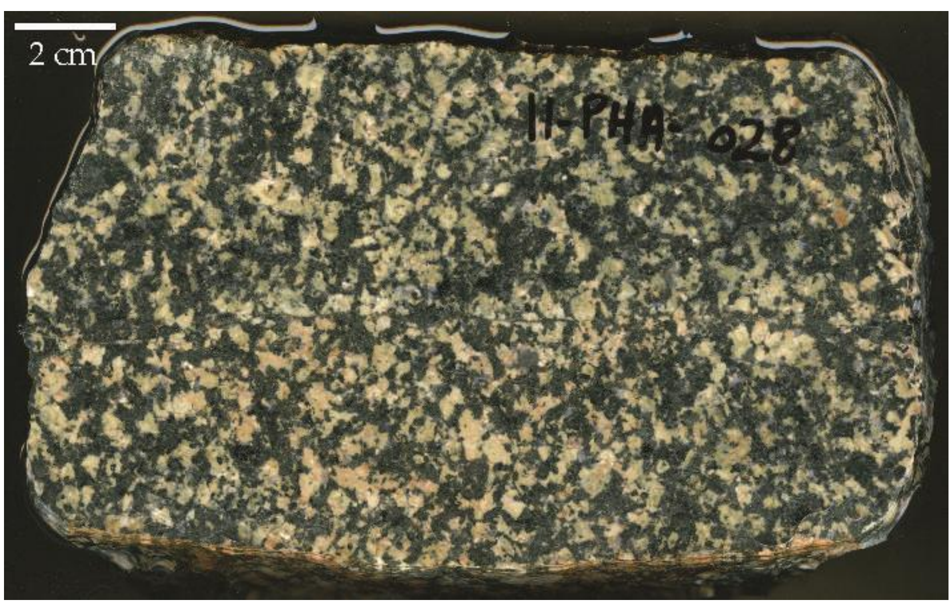

Figure 12. Sawn hand sample 11PHA-28.

11PHA-28 (diorite) The specimen, nondeformed, is a hornblende-plagioclase-biotite cumulate with interstitial quartz + amphibole + apatite + zircon. Apatite is unusually abundant and forms euhedral inclusions in ferromagnesian phenocrysts as well as interstices. Primary amphibole is substantially replaced by a green secondary amphibole.

Figure 13. Outcrop (wet) of orbicular gabbro, 11PHA-36.

11PHA-36A (gabbro) The outcrop is a striking nondeformed, orbicular leucogabbro. The orbicule cores are green-weathering with a cm-scale white rim and a mesocratic interstitial material. In thin section, the orbicules (average 3 cm diameter) are cored by very pale green chlorite plus a moderately birefringent, near-colorless sheet silicate (likely phlogopite) with relic orthopyroxene, plus minor epidote and muscovite after plagioclase. The rims are dominated by altered plagioclase; the material between the orbicules is hornblende + plagioclase + quartz. Opaque minerals are present in trace quantity and may be entirely secondary. All minerals have random orientations and alteration likely occurred by H_2O-dominated, late magmatic fluids.

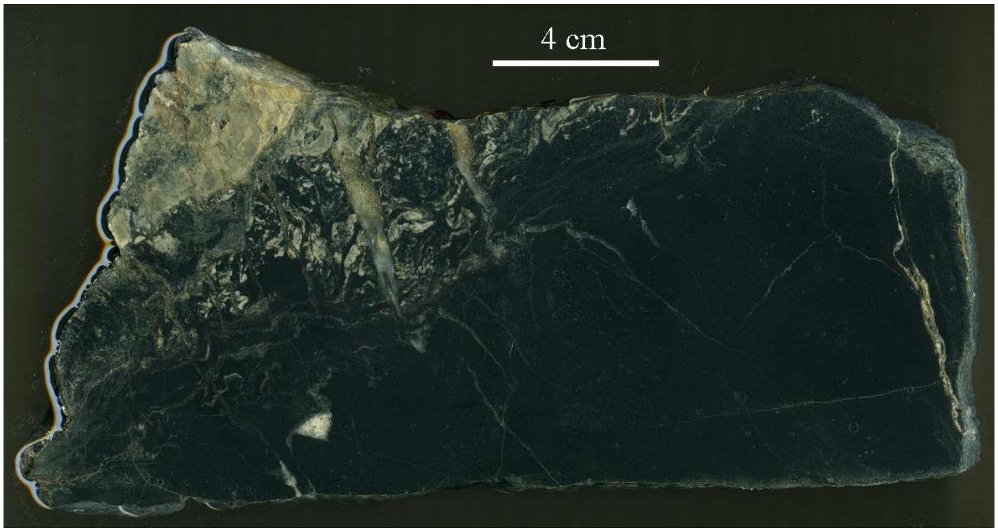

Figure 14. Sawn hand sample of basalt 11JP271A01B

11JP271A01B (Ol-normative basalt) The sample, nondeformed, is taken from the top of a flow; the upper contact exhibits flow breccia and extensional fractures filled with chert.

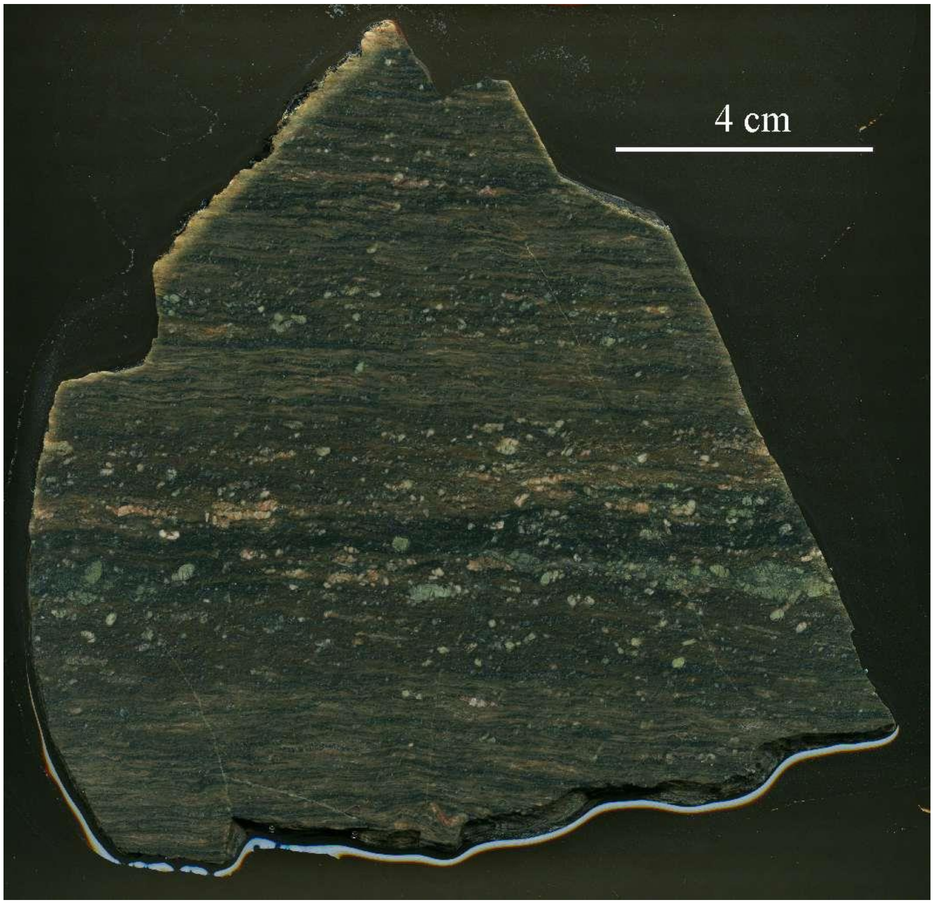

Figure 15. Sawn hand sample of porphyry 11JP520A02

11JP520A02 (quartz-feldspar porphyry) The sample is strongly foliated with about 3:1 extension lineation. This sparsely crystalline quartz-feldspar porphyry (<10%) has a fine-grained dark matrix enclosing flattened leucocratic lapilli. The compositional layering represented by different abundances of phenocrysts and different colour bands has been transposed parallel to schistosity and refolded at least twice, as has the compositional layering in the Amer Group (Calhoun et al., 2014). The numerous leucocratic, mm-scale, strongly flattened lapilli may include infilled vesicles.

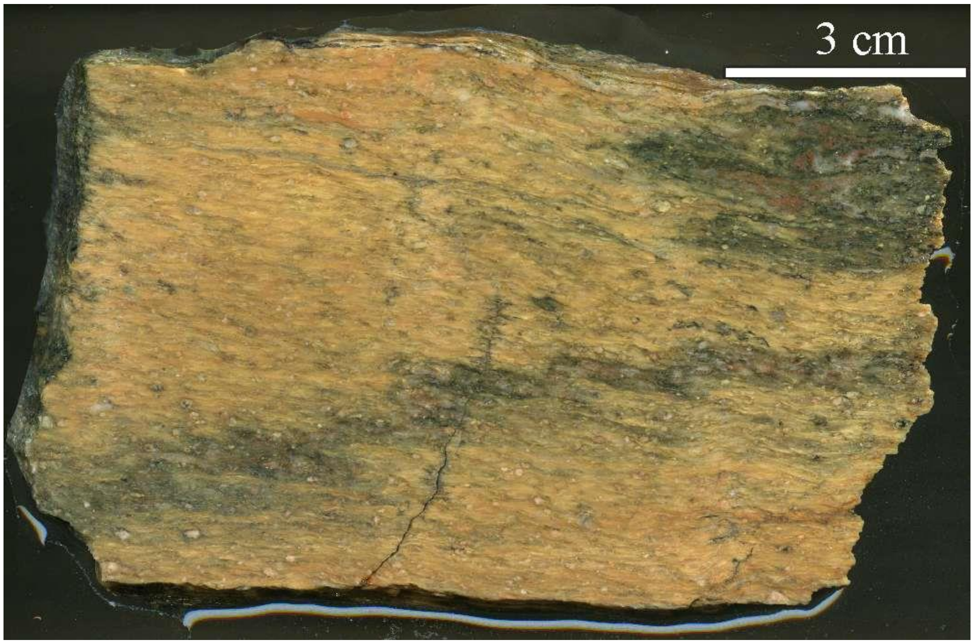

Figure 16. Sawn hand sample of porphyry 11JP045A03B

11JP045A03B (quartz-feldspar porphyry) The sample is a strongly foliated rhyolite with subequal quartz and feldspar flattened and extended into long ribbons, extension lineation and C\S fabric as for 11JP520 above.

Geochemistry

The analytical data are in the Appendix (whole rock geochemistry), with the Nd isotopic data in Table 1. Hand samples selected for whole rock geochemical analyses were trimmed of weathered surfaces. The samples were crushed using a Braun Chipmunk and pulverized in a Rock Labs Ltd. shatterbox using a carbon steel mill head. Major and trace elements were analyzed at Acme Analytical Laboratories (Vancouver) Ltd., using the 4A-4B whole rock lithogeochemical package with major elements determined by x-ray fluorescence (XRF) and trace elements determined by inductively coupled mass spectrometry (ICP-MS) after standard fusion and digestion techniques. Data accuracy was evaluated by submission of two standards. A subset of the sample suite was selected for Sm-Nd isotopic analysis by contract (laboratory of B. Cousens, Carleton University; R. Mitchell, analyst).

Geochemical Groupings

The analyses were divided into 5 groups and one subgroup (group membership is noted in the accompanying spreadsheet) based on chondrite-normalized REE profiles (Fig. 17) and MORB-normalized multielement plots (Fig. 18). The resulting groups correlate strongly with normative Qz content, and display some systematic variations that can be attributed at least in part to crystal fractionation.

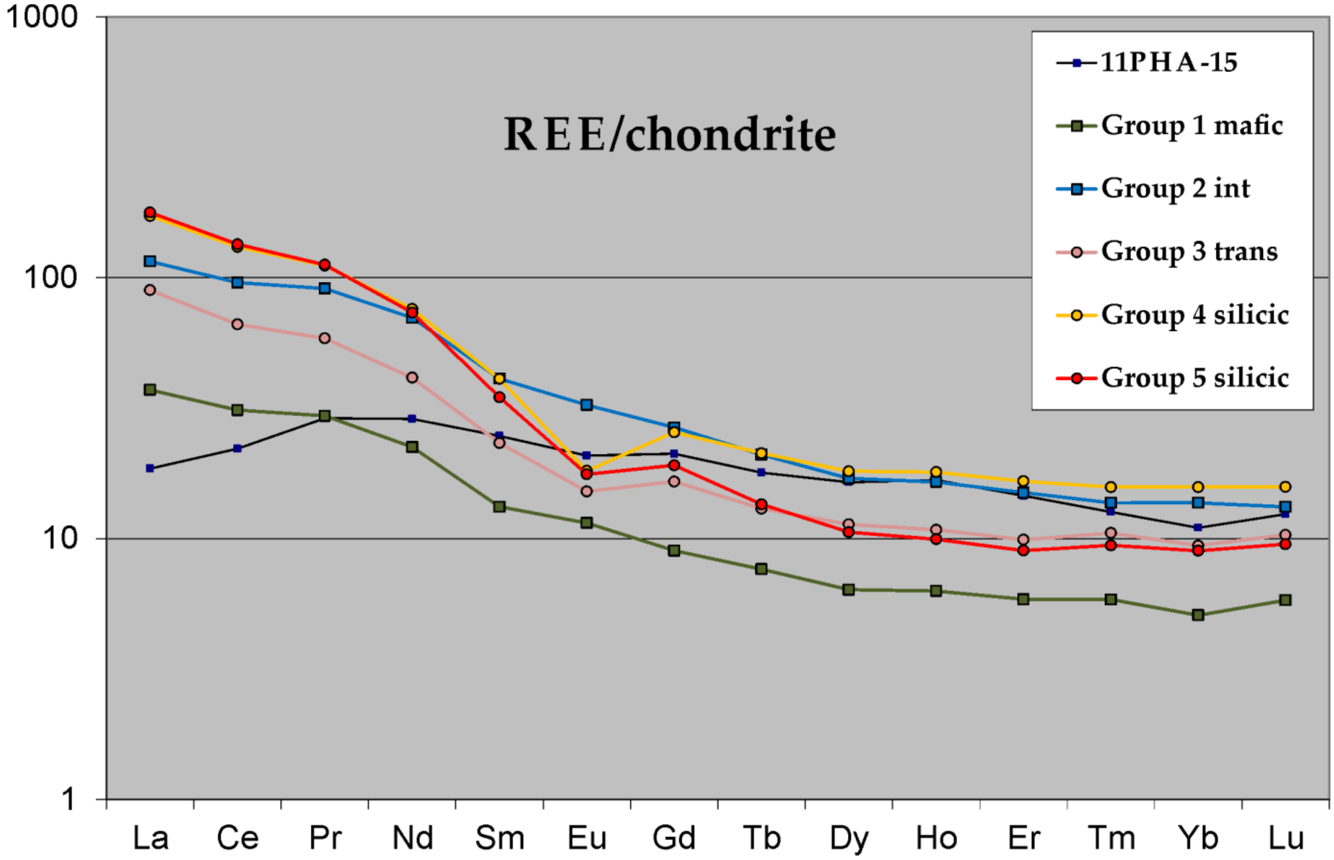

Figure 17. Averages of compositional groups, normalized to chondrites (values of Nakamura, 1974). The Ne-normative amphibole cumulate 11PHA-15 is included.

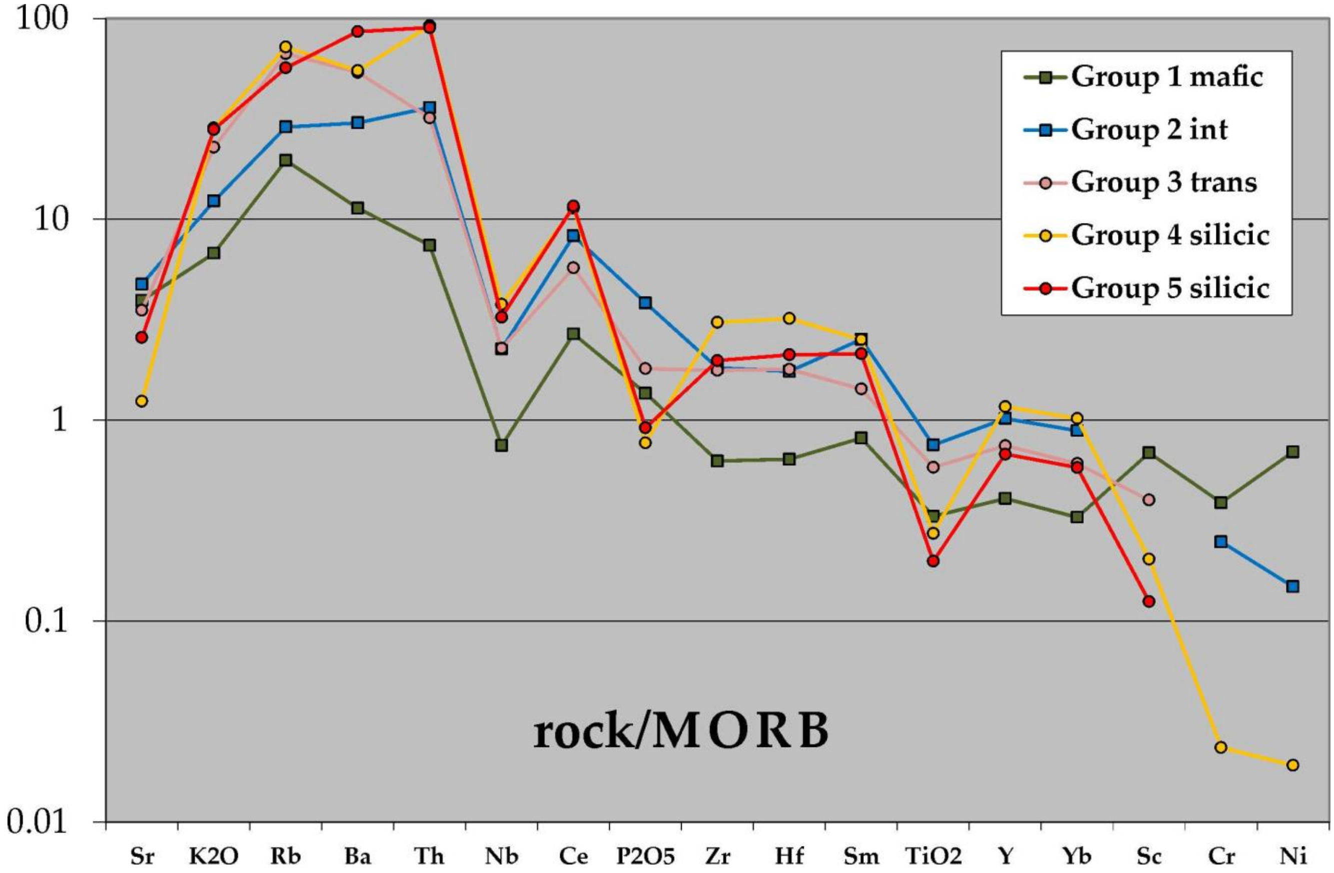

Figure 18. Averages of compositional groups, normalized to MORB (after Pearce, 1983).

Group 1: mafic rocks (n=6)

This group includes all Ol-normative rocks, plus one sample with Qz<0.5%. One sample is Ne-normative; two are extrusive rocks and the remainder are coarse-grained intrusive rocks. The average REE profile is similar to Phanerozoic to modern tholeiitic continental basalts (La_{cn}=37, Lu_{cn}=5.8). A slight upward concavity in MREE may be a result of amphibole fractionation. The multielement plot shows negative anomalies in Nb (pronounced) and Ti (modest).

One Ne-normative rock (11PHA-15, 2.8% Ne) resembles the mafic group and is petrographically identical to it but is anomalous for having a concave-down REE profile with marked depletion in La through Sm. The outcrop this was collected from is a hornblende cumulate, which contains numerous tonalite segregations, and the anomalous REE pattern likely reflects the REE content of the amphibole, and migration of LREE-rich tonalite melt.

Group 2: intermediate rocks (n=5)

This group includes all rocks classified as diorites based on normative 0.5<Qz<20. Mineralogically and texturally, they grade into the group 1 mafic gabbros. In the multielement plot, they appear very similar to the mafic group 1 but are higher in incompatible elements, particularly Th, and depleted in compatible elements (crossover at Sc). Average overall REE contents are significantly higher than group 1 (average La_{cn} =115) but parallel to it, with no Eu anomaly. The two groups can easily be related by fractionation of olivine and pyroxene. However, the average REE content of group 2 is *higher* than that of the transitional group 3 and is comparable to the silicic group 4. This is consistent with the mafic and intermediate groups representing a different magma source than the more silicic groups: crystal fractionation did not carry through to generate the silicic rocks.

Group 3: transitional rocks (n=3)

This group includes three norm-defined diorites that are similar to the intermediate group in major element composition, but which display modest negative Eu anomalies. All three are extrusive rocks from the same station (11JP-271). This group has markedly lower REE than the intermediate group and cannot be related to it by crystal fractionation or crustal contamination. However, it resembles the intermediate group in the multielement plot, except for elevated K, Rb, and Ba, with a modest negative P anomaly.

Group 4: silicic rocks (n=12)

This group includes three intrusive rocks that were norm-classified as granodiorite, plus 8 rhyolites field classified as quartz-feldspar porphyries, quartz porphyry, rhyolite lapilli tuff, and rhyolite, all with Qz>30. This group has a marked negative Eu anomaly and the highest overall HREE concentrations in the sample suite; LREE are higher than all other groups except group 5. In the multielement plot, IE are markedly enriched over groups 1-3 and strong negative anomalies in Nb, P, and Ti are present.

Group 5: fractionated silicic rocks (n=4)

This group consists entirely of extrusive rocks: three quartz-feldspar porphyries and one rhyolite, all with Qz>30. This group differs from group 4 in having a more strongly fractionated REE profile, with LREE equal to the silicic group 4. The multielement profiles of the two groups are essentially identical.

Unclassified samples

Five silicic rocks have anomalous characteristics. Sample 09JP-038B01 (phyllitic felsic tuff) is a Qz-rich rock but has a modest negative Eu anomaly and overall REE contents similar to the transitional group; it may be a silicified andesite or dacite. Samples 11JP045A03 and A05 have relatively low overall REE contents (similar to the transitional group) with large negative Eu anomalies, and are distinguished by large negative Ba anomalies in the multielement plot. They are probably a variant of the fractionated silicic group 5 (the two other samples from station 11JP045 are within that group) which additionally underwent fractionation of potassium feldspar. They are therefore assigned to a subgroup 5a.

Sample 11JP395A02 (quartz-feldspar porphyry) has a strongly fractionated REE pattern but very low overall REE contents (less than the mafic group for REE heavier than Nd) and no Eu anomaly. Sample 09JP039A01 (mylonitized granite) is similarly fractionated, with no Eu anomaly, though with higher overall concentrations. Neither is distinguished in the multielement plot. The absence of an Eu anomaly in rocks with strongly fractionated REE patterns is problematical. These samples may have been misidentified as members of the SIS, but more data would be required to demonstrate their exclusivity.

Sm-Nd isotopes

The Nd isotope geochemistry of silicic intrusive rocks of the SIS has been measured in numerous studies. A compilation of 59 analyses throughout the Rae Province by Peterson et al. (2010) has an average depleted mantle model age (T_{DM}) of 2855 Ma, and a range of 2654-3626 Ma. These values are consistent with generation by partial melting of older crustal rocks. Therefore, we prioritized our Sm-Nd analyses in this study to the mafic rocks (gabbro and diorite), which were previously unstudied. Four samples were submitted for Sm-Nd isotope analysis under contract to Carleton University (laboratory of B. Cousens, R. Mitchell analyst) (Table 1). One sample (11PHA-28), which was repeated, produced highly anomalous results with an extreme value of $\varepsilon_{Nd,CHUR}$ (<-35) and depleted mantle model ages much greater than 4.5 Ga. This intrusive sample, which was field classified as a potassium feldspar porphyritic monzonite, has a composition that places it in group 2 (intermediate, dioritic). A reassessment suggests it may be a mixture of mafic and porphyritic silicic magmas. Sample 11PHA-15, which is an amphibole cumulate with anomalous REE profile, also generated unusual, but physically more plausible values with ε_{Nd}=+14.7. The high positive value may be related to removal of a quartz tonalite segregation, and the observed LREE depletion.

Samples 11PHA-7 and 11PHA-36A, which have no anomalous geochemical characteristics, produced results consistent with extraction from depleted asthenospheric mantle at 2.6 Ga ($\varepsilon_{Nd,2.6Ga}$ =+2.2 and +2.7, respectively) and with T_{DM}=2639 and 2601 Ma. More analyses will be needed before these can be convincingly interpreted; however, these initial results indicate that some of the mafic rocks in our data set represent magmas extracted from convecting mantle at the time of their emplacement. They also emphasize that the mafic rocks of Group 1 have a different source than silicic members of the SIS.

Table 1: Sm-Nd isotope analyses

sample	Sm	Nd	$^{147}Sm/^{144}Nd$	$^{143}Nd/^{144}Nd$	Nd(T)	ε_{Nd}	T_{DM}
11PHA-7	2.59	13.64	0.114710	0.511342	0.509375	2.2	2639
11PHA-15	4.12	18.06	0.137831	0.512378	0.510014	14.7	1334
11PHA-36A	0.85	4.90	0.105336	0.511207	0.509400	2.7	2601
11PHA-28	8.25	43.49	0.114600	0.509342	0.507377	-37.1	6092

Depleted mantle model ages (TDM) after DePaolo, 1981.

Discussion

The Zr/Ti vs Nb/Y diagram (Fig. 19) can distinguish igneous series on the basis of alkalinity. All of our samples plot on the low Nb/Y side of subalkaline rocks, consistent with a primary magma type similar to tholeiite basalt, and in accord with the presence of preserved orthopyroxene in one gabbro. Three fractionated silicic rocks, including the two from subgroup 5a with depleted Ba, have distinctively higher Nb/Y, which confirms their distinction from the remainder of the silicic samples.

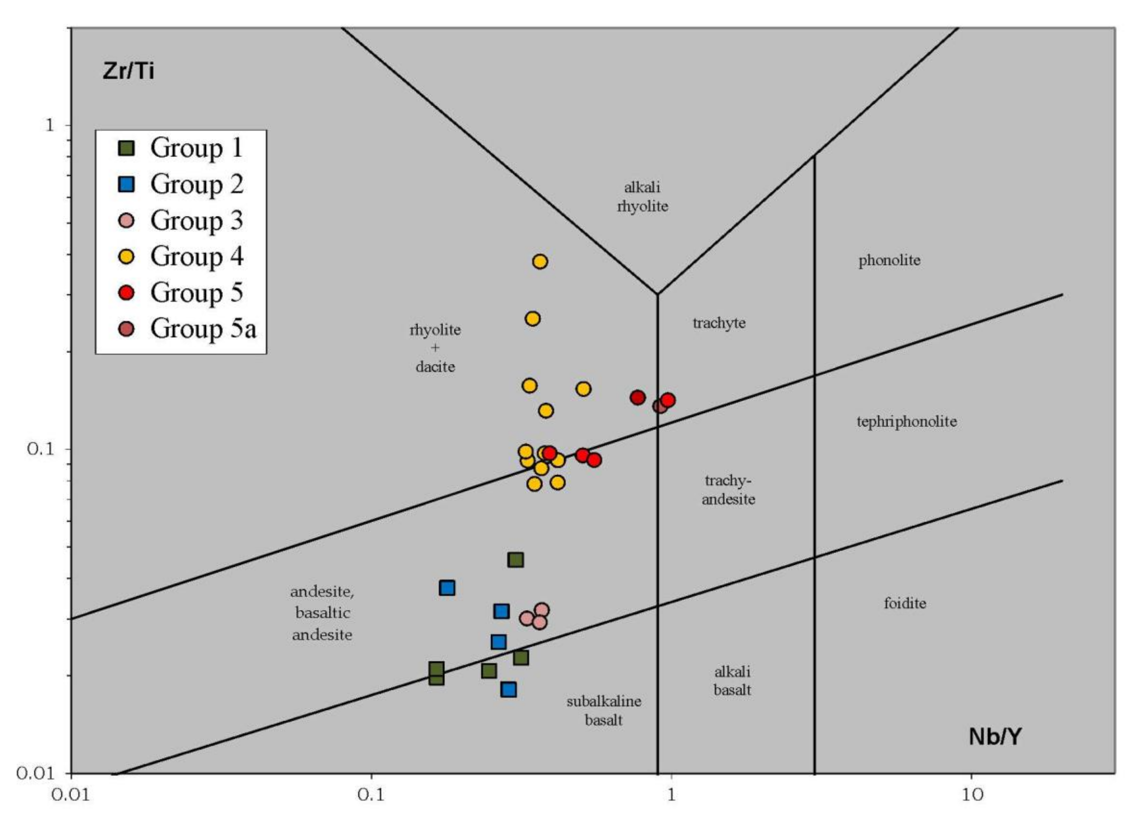

Figure 19. Modified Winchester-Floyd diagram (after Pearce, 1996).

This diagram reproduces the mafic-felsic gap in isotopic compositions. The increasing negative Eu, Ti, and P anomalies within the felsic series is consistent with fractionation of plagioclase, oxides, and apatite, and finally with alkali feldspar to produce the Ba-depleted Group 5a.

The MORB-normalized plots (Fig. 18) all show marked negative anomalies in Nb and modest to strong negative anomalies in other HFSE, with significant enrichment in IE that reaches a maximum at K-Rb-Ba-Th. This pattern is often attributed to magma genesis at destructive plate margins and could lead one to conclude that the SIS represents a continental arc or similar phenomenon. However, Paleoproterozoic igneous suites in the western Churchill Province (Hudson Suite, Dubawnt minettes, and Nueltin Granite) display the same pattern, and these are post- to anorogenic suites that erupted within crust far removed from any active subduction zone. It is probable that the silicic members of the SIS are melts of older crust that formed at convergent margins (before amalgamating at up to ca. 2.7 Ga), and which acquired their trace element patterns from their sources.

The Ga/Al ratio of silicic rocks is an indicator of an origin in granulitic lower crust affected by a previous episode of melt extraction, with the boundary separating anorogenic granitic melts from, e.g., I-type granites, occurring at 1.8895x(Ga,ppm)/(%Al_2O_3)=2.6 (Whalen et al., 1987). The average value of groups 3 through 5 is 2.57 (range 1.61-2.92), consistent with a potential relation of silicic SIS and Pukiq Formation magmas to melting of granulitic lower crust.

The origin of the mafic magmas is unclear at this time. The convergent plate margin incompatible element signature may have been acquired through interaction with crustal rocks, or may be an authentic subduction-related signature in the source region. Additional data will be needed to address these questions.

Acknowledgments

Geological mapping by Brian McEwan and introductions to the geology in the Meadowbank River area by Bruce Kjarsgaard and Sally Pehrsson made large contributions to our knowledge of the Snow Island Suite and related volcanic rocks. Geophysical discussions with Victoria Tschirhart, Mike Thomas, Bill Morris and Warner Miles provided considerable insights on the third dimension. John Percival and Rob Berman shared their knowledge of the SIS north and west of the Amer Mylonite Zone, Bill Davis helped understand geochronological data and their geological context, and Tony LeCheminant shared his knowledge of samples and type localities across the Tebesjuak Lake, Aberdeen Lake and Schultz Lake map areas. Able field assistance and office support by Jeffrey Scott, Chris Stieber, Bianca D'Aoust, Warren Riemer and Peter Tschirhart were much appreciated. Logistical support was provided by Ookpik Aviation and Forest helicopters, contracted via Polar Continental Shelf Project. Accommodation was at Baker Lake Lodge managed by Boris Kotelewetz and Helen Foster. The manuscript benefitted from critical review by Bruce Kjarsgaard.

References

Ashton, K.E., 1988. Precambrian geology of the southeastern Amer Lake area (66H/1), near Baker Lake, N.W.T. PhD thesis, Queen's University, Kingston, Ontario, 335 p.

Calhoun, L., White, J.C., Jefferson, C.W., Patterson, J., and Tschirhart, V., 2014. Integrated geodatabase study of the complexly deformed U-hosting Paleoproterozoic Amer Group, Nunavut. Geological Survey of Canada, Scientific Presentation 19, 26 pages, doi:10.4095/293108.

Corrigan, D., Nadeau, L., Brouillette, P., Wodicka, N., Houle, M.G., Tremblay, T., Machado, G., and Keating, P., 2013. Overview of the GEM Multiple Metals – Melville Peninsula project, central Melville Peninsula, Nunavut. Geological Survey of Canada Current Research 2013-19.

Davis, W.J., Berman, R.G., and MacKinnon, A. 2013. U-Pb geochronology of archival rock samples from the Queen Maud Block, Thelon Tectonic Zone and Rae Craton, Kitikmeot region, Nunavut, Canada. Geological Survey of Canada Open File 7409.

Davis, W.J., Berman, R.G., Nadeau, L., and Percival, J.A., 2014. U-Pb zircon geochronology of a transect across the Thelon tectonic zone, Queen Maud region, and adjacent Rae craton, Kitikmeot Region, Nunavut, Canada; Geological Survey of Canada, Open File 7652, 1 .zip file. doi:10.4095/295177

Davis, W.J., Pehrsson, S.J., and Percival, J.A. 2015. Results of a U-Pb zircon geochronology transect across the southern Rae craton, Northwest Territories, Canada. Geological Survey of Canada Open File 7655.

DePaolo, D.J., 1981. A neodymium and strontium isotopic study of the Mesozoic calc-alkaline granitic batholiths of the Sierra Nevada and Peninsular Ranges, California. Journal of Geophysical Research 86, 10470-10488.

Hadlari, T., Rainbird, R. H., and Pehrsson, S. J., 2004. Geology, Schultz Lake, Nunavut. Geological Survey of Canada, Open File 1839, 1 sheet, scale 1:250 000.

Hinchey, A.M., Davis, W.J., Ryan, J.J., Nadeau, L., 2011. Neoarchean high-potassium granites of the Boothia mainland area, Rae domain, Churchill Province. U-Pb zircon and Sm-Nd whole rock isotopic constraints. Canadian Journal of Earth Sciences 48, 247-279.

Jefferson, C., Pehrsson, S., Peterson, T., Chorlton, S., Davis, B., Keating, P., Gandhi, S., Fortin, R., Buckle, J., Miles, W., Rainbird, R., Lecheminant, T., Tschirhart, V., Tschirhart, P., Morris, W., Scott, J., Cousens, B., McEwan, B., Bethune, K., Riemer, W., Calhoun, L., White, J., MacIsaac, D., Leblon, B., Lentz, D., LaRocque, A., Shelat, Y., Patterson, J., Enright, A., Stieber, C., Riegler, T., 2011a. Northeast Thelon region geoscience framework - new maps and data for uranium in Nunavut. Geological Survey of Canada Open File 6950.

Jefferson, C.W., Chorlton, S.J., Pehrsson, S.J., Peterson, T.D., Wollenberg, P., Scott, J., Tschirhart, V., McEwan, B., Bethune, K., Calhoun, L., White, J.C., Leblon, B., LaRocque, A., Shelat, Y., Lentz, D., Patterson, J., Riegler, T., Skulski, T., Robinson, S., Paulen, R., McClenaghan, M.B., Layton-Matthews, D., MacIsaac, D., Riemer, W., Stieber, C., Tschirhart, P., 2011b. Northeast Thelon Region: geomapping for uranium in Nunavut. Geological Survey of Canada Open File 6962.

Jefferson, C.W., Pehrsson, S.J., Peterson, T., Tschirhart, V., Anand, A., Wollenberg, P., LeCheminant, A.N., Riegler, T., Bethune, K., Chorlton, L.B., McEwan, B., Tschirhart, P., Scott, J.M.J., Davis, W., McNicoll, V., Riemer, W., Patterson, J., Morris, W.A., and Stieber, C.; 2015a: Outcrop and remote predictive geology of the western Marjorie–Tehek supracrustal belt and Northeast Thelon Basin margin in parts of NTS 66A and 66B, Nunavut. Geological Survey of Canada, Open File 7241, 1 CD-ROM.

Jefferson, C.W., White, J.C., Young, G.M., Patterson, J., Tschirhart, V., Pehrsson, S.J., Calhoun, L., Rainbird, R.H., Peterson, T., Davis, W.J., Tella, S., Chorlton, L.B., Scott, J.M.J., Davis, W.J., Percival, J.A., Morris, W.A., Keating, P., Anand, A., Shelat, Y. and MacIsaac, D., 2015b: Outcrop and remote predictive geology of the Amer Belt and basement beside and beneath the northeast Thelon Basin in parts of NTS 66A, B, C, F, G and H, Nunavut. Geological Survey of Canada, Open File 7242, 1 CD-ROM.

Kjarsgaard, B.A., Kerswill, J.A., and Jenner, G.A., 1997. Lithostratigraphy and metallogenic implications of komatiite - banded iron formation - felsic volcanic rocks of the Archean Woodburn Lake group, Pipedream lake, central Churchill Province, Northwest Territories. Geological Survey of Canada Current Research 1997-C, 101-110.

LeCheminant, A.N., Ianelli, T.R., Zaitlin, B., and Miller, A.R., 1981. Geology of Tebesjuak Lake map area, District of Keewatin : a progress report. Geological Survey of Canada Paper 81-01B, 113-128.

LeCheminant, A.N., and Roddick, J.C., 1991. U-Pb zircon evidence for widespread 2.6 Ga felsic magmatism in the central District of Keewatin, N.W.T. *in* Radiogenic Age and Isotopic Studies: Report 4; Geological Survey of Canada Paper 90-2, 91-99.

LeCheminant, A.N., Jackson, M.J., Galley, A.G., Smith, S.L. and Donaldson, J.A., 1984: Early Proterozoic Amer Group, Beverly Lake map area, District of Keewatin. in Current Research, Part B, Geological Survey of Canada, Paper 84-1B, p. 159-172.

McEwan, B., 2012: Structural style and regional comparison of the Paleoproterozoic Ketyet River group in the region north-northwest of Baker Lake, Nunavut. M.Sc. thesis, The University of Regina, 121p + appendices.

Nakamura, N. 1974. Determination of REE, Ba, Fe, Mg, Na, and K in carbonaceous and ordinary chondrites. Geochimica et Comochimica Acta, **38**: 757–775.

Pearce, J.A., 1983. Role of the sub-continental lithosphere in magma genesis at active continental margins. In: C.J. Hawkesworth, M.J. Norry (eds.), Continental basalts and mantle xenoliths. Birkhauser Boston, Cambridge, Massachusetts, pp. 230-249

Pearce, J.A., 1996. A user's guide to basalt discrimination diagrams. In: D.A. Wyman (ed.), Trace element geochemistry of volcanic rocks: applications for massive sulphide exploration. Geological Association of Canada Short Course Notes v. 12, pp. 79-113.

Pehrsson, S.J., Berman, R., and Davis, W.J., 2013. Paleoproterozoic orogenesis during Nuna aggregation: a case study of reworking of the Archean Rae craton, Woodburn Lake, Nunavut. Precambrian Research, 232, 167-188, http://dx.doi.org/10.1016/j.precamres.2013.02.010.

Peterson, T.D., and Lee, C., 1995. Pre-Dubwant plutonism and deformation in the Nicholson Lake-Dubawnt Lake area, Northwest territories. Geological Survey of Canada Current Research 1995-C, 11-18.

Peterson, T.D., 2006. Geology of the Dubawnt Lake area, Nunavut-Northwest Territories. Geological Survey of Canada Bulletin 580.

Peterson, T.D., Pehrsson, S., Skulski, T., Sandeman, H.A., 2010. Compilation of Sm-Nd isotope analyses of igneous suites, western Churchill Province. Geological Survey of Canada Open File 6439.

Peterson, T.D., Scott, J.M.J., LeCheminant, A.N., Chorlton, L., D'Aoust, B., 2014. Geology, Tebesjuak Lake area (NTS 65O). Geological Survey of Canada Canadian Geoscience Map 158.

Rainbird, R.H., Davis, W.J., Pehrsson, S.J., Wodicka, N., Rayner, N., and Skulski, T. 2010: Early Paleoproterozoic supracrustal assemblages of the Rae domain, Nunavut, Canada: Intracratonic basin development during supercontinent break-up and assembly. Precambrian Research, v 181, p. 167-186.

Schau, M., Tremblay, F. and Christopher, A., 1982. Geology of Baker Lake map area, District of Keewatin: a progress report. in Current Research, Part A, Geological Survey of Canada, Paper 82-1A, p. 143-150.

Tella S., 1994, Geology, Amer Lake (66 H), Deep Rose Lake (66 G), and parts of Pelly Lake (66 F). Geological Survey of Canada Open File 2969, 1 sheet, scale 1:250 000.

Thomas, M.D., 2012: Shallow Crustal Structure in Meadowbank River - Tehek Lake area: Insights from Gravity and Magnetic Modelling. Geological Survey of Canada, Open File 7308, 42 p. doi: 10.4095/292157.

Tschirhart, P.A., Morris, W.A., and Jefferson, C.W., 2013a: Geophysical modeling of the Neoarchean Woodburn Lake and Paleoproterozoic Ketyet River groups, and plutonic rocks in central Schultz Lake map area, Nunavut. Geological Survey of Canada, Current Research 2013-2; 19 p. doi:10.4095/292116.

Tschirhart, V., Morris, W.A., Jefferson, C.W., 2013b: Framework geophysical modelling of granitoid vs. supracrustal basement to the northeast Thelon Basin around the Kiggavik uranium camp, Nunavut. Canadian Journal of Earth Sciences, 50, 667-677,. dx.doi.org/10.1139/cjes-2012-0149.

Whalen, J.B., Currie, K.L., Chappel, B.W., 1987. A-type granites: geochemical characteristics, discrimination and petrogenesis. Contributions to Mineralogy and Petrology 95, 407-419.

Zaleski, E., 2005: Geology, Meadowbank River area, Nunavut. Geological Survey of Canada, Map 2068A, scale 1:50,000.